

## **DIRECT NUMERICAL SIMULATIONS AND EXPERIMENTS OF A DENSE GAS-FLUIDIZED BED**

**Y. TANG<sup>\*</sup>, N.G. DEEN, E.A.J.F. PETERS and J.A.M. KUIPERS**

Multiphase Reactors Group, Department of Chemical Engineering and Chemistry, Eindhoven University of Technology, P.O. Box 513, 5600MB Eindhoven, The Netherlands

<sup>\*</sup>Corresponding author, E-mail address: y.tang2@tue.nl

### **ABSTRACT**

We report our study on fluidization of 5000 spherical particles in a pseudo-2D gas-fluidized bed by direct numerical simulations (DNS) and experiments as well. DNS are performed using an immersed boundary method, together with the methodology developed in our earlier work for accurate prediction of gas-solid interactions at relatively low grid resolutions. Experimental measurements of solids mean motion are conducted using a combined particle image velocimetry (PIV) and digital image analysis (DIA) technique. Furthermore, the PIV technique is extended and applied for instantaneous measurements of the particle granular temperature, which is a key characteristic of particle velocity fluctuations.

This paper presents a detailed direct comparison between IBM simulation results and experimental data for realistic gas fluidization, which has not been reported before in literature. The comparison reveals a good agreement with respect to the time-averaged solids motion, as well as the fluctuations of the pressure drop over the bed. The granular temperatures calculated from the simulations also agree very well with the experimental data measured by the extended PIV technique.

### **NOMENCLATURE**

$d_m$	diameter for the marker points distribution
$d_p$	particle diameter
$h$	grid size
$n_p$	number of particles
$t$	time
$u_g$	superficial gas velocity
$u_{mf}$	minimal fluidization velocity
$x$	bed width along horizontal direction
$z$	bed height along vertical direction
$\mathbf{v}$	particle velocity
$\Delta P$	pressure drop
$\Phi$	solids volumetric flux
$\theta$	particle granular temperature

### **INTRODUCTION**

Gas-fluidized beds are widely applied in the chemical and process industries for mixing, coating, drying, catalytic and non-catalytic reactions, and many other applications. Owing to their favourable characteristics such as excellent mixing and heat/mass transfer, gas-fluidized beds have been the subject of extensive research campaigns.

There exists a vast amount of literature on experimental investigation of transport phenomena in gas-fluidized beds. Over the years, many techniques have been developed to perform measurements in such systems. Particle Image Velocimetry (PIV) and Digital Image Analysis (DIA) are two of the most common non-invasive techniques applied to analyse the instantaneous solids motion and to study gas bubbles' behaviour, respectively. Laverman et al. (2008) combined PIV and DIA techniques to correct for the influence of particles raining through the roof of the bubbles on the measured time-averaged solids velocity profiles. Recently reported work (Dang et al., 2013; Patil et al., 2015) have combined PIV and DIA with infrared thermography to study the mass and heat transfer characteristics in gas-fluidized beds. In addition, a very important parameter to characterize dense gas-solid flows is the granular temperature, which characterizes the kinetic energy associated with the random particle velocities. Holland et al. (2008) and Müller et al. (2008) reported time-averaged measurements of the granular temperature in gas-fluidized beds using a magnetic resonance (MR) technique, and found fair agreement to their simulation results. Dijkhuizen et al. (2007) extended the PIV technique to enable simultaneous measurements of instantaneous velocity and granular temperature fields in dense gas-fluidized beds. This extended PIV technique was demonstrated for a bubble forming and rising in the bed and a freely bubbling fluidized bed. So far, no further work has been reported that utilizes this technique.

Despite numerous experimental investigation, quantitative understanding of the flow behaviour in gas-fluidized beds remains challenging. In this respect, computational fluid dynamics (CFD) simulations can, in many cases, complement experimental studies by providing detailed information that is difficult to obtain otherwise. Researchers have developed a variety of CFD models that describe gas-solid flows at different levels of details (van der Hoef et al., 2008). Among those models, Direct Numerical Simulation (DNS) is the most detailed model, in which the incompressible Navier-Stokes (NS) equations are solved for the gas phase whereas the Newtonian equations of motion are solved for each individual particle, coupled with appropriate boundary conditions imposed at the particle surface. Naturally, DNS is the most detailed model to study fluid dynamics in fluidized beds, from which the results can be used to improve the larger-scale models. However, owing to the complexity of particle-flow interactions, direct numerical simulations of inertial particulate flow with finite-size particles have often been restricted to a small number of particles. This

means that DNS of fluidization is prohibitively expensive even for fluidized beds at the lab scale, where the number of particles is in the order of thousands.

Together with the rapid increase of computing power, parallel implementation of DNS-type methods opens an interesting option to study gas-solid suspensions with a relatively large number of particles. Nevertheless, direct numerical simulations of fluidization in realistic systems are very rarely reported, due to the complex gas-solid interactions in comparison with sedimentation or segregation of particles by gravity. Pan et al. (2002) did simulate the fluidization of 1024 spheres in liquids at finite Reynolds numbers of  $O(1000)$ , and compared the results with an experiment. Also, Deen et al. (2012) performed DNS of liquid fluidization of 1296 spheres to study the fluid-particle heat transfer characteristics. Fluidization of 400 spheres in a gas-fluidized bed was simulated by Kuwagi et al. (2010) using a volumetric-type immersed boundary (IB) method, in which inhomogeneous gas flow was observed in the particle bed. Kriebitzsch et al. (2013) compared DNS with DEM simulations of a small gas-fluidized bed consisting of 2000 particles, which showed some discrepancy with respect to the computed gas-solid interaction force. Finally, the latest DNS of fluidization reported in literature was a study of the heat transfer of 225 heated spheres in a gas-fluidized bed (Feng et al., 2014).

With respect to the DNS-type IB method, we have developed a methodology (Tang et al., 2014) that allows for highly accurate simulations of dense gas-solid flows at relatively low resolutions. This can efficiently reduce the computational cost of simulations and accordingly make it feasible for, e.g., modelling fluidization in a realistic system. Consequently, a direct comparison between DNS and experiments of fluidized beds is possible. This will be demonstrated in this work for DNS of fluidization of 5000 spherical particles in a small pseudo-2D gas-fluidized bed. The simulation results will be directly compared with experimental measurements conducted in a lab set-up using the extended PIV (Dijkhuizen et al., 2007) and DIA techniques. Detailed comparisons are reported for pressure drop fluctuations over the bed, bed expansion, time-averaged solids velocity field, as well as the granular temperature. This paper is organized as follows: First, the immersed boundary method and the two experimental measuring techniques are introduced; Next, the modelled/experimental set-up is illustrated; Subsequently, detailed comparisons between experimental data and simulation results are presented; Conclusions are given at the end of this paper.

## IMMERSED BOUNDARY METHOD

Direct numerical simulations in this work refer to the most detailed model in the multiscale modelling scheme introduced by van der Hoef et al. (2004) for an industrial scale fluidized bed. In this DNS model, the gas phase is solved on a grid smaller than the size of the particles, and the solid phase is described by individual particles with their interaction with the gas phase modelled by employing boundary conditions at the surface of the particle. An immersed boundary method (IBM) is adopted to perform DNS of a gas-fluidized bed in this work. Implementation details of this method can be found in Tang et al. (2014), and only a brief outline is given here.

A schematic explanation of the IBM methodology is presented in Figure 1. The gas phase is governed by the NS equations, which are solved on a fixed and structured Eulerian grid with its grid size  $h$  smaller than the particle diameter  $d_p$ . These equations are solved using state-of-the-art CFD methods, where second-order schemes are used for space and time discretization of the momentum equations, in which the convective, viscous, and pressure terms are treated in an explicit, semi-implicit and implicit manner, respectively. For the solids phase, each particle is represented by a set of marker points that are distributed over a sphere of diameter  $d_m$ . A hard-sphere model is used for the particle-particle and particle-wall interactions, where the collisions are considered binary, instantaneous and non-ideal. The motion of particles follows Newton's second law, from which the translational and rotational velocities are updated every CFD time step.

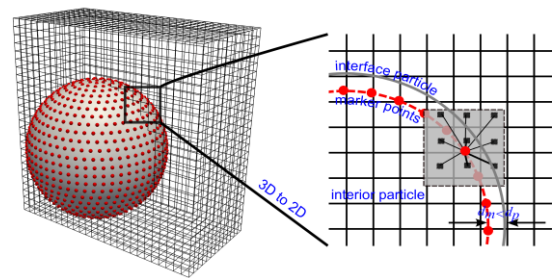


**Figure 1:** Schematic explanation of the IBM: representation of an immersed particle on a Cartesian grid by a set of marker points (left), the interpolation and extrapolation of quantities between a marker point and grid points (right).

Additionally, the gas-solid coupling is taken into account by adding a force term into the NS equations. This force term is computed at each marker point such that the local gas phase velocity is equal to the surface velocity at this location of the marker point. Thereby, the no-slip boundary condition is enforced at the surface of the particle. The sum of this force term originating from the marker points of one particle equals the total force that the particle exerts on the gas. A regularized delta function suggested by Deen et al. (2004) is employed for the communication between marker points and adjacent Eulerian grid points, which takes places with a support of  $3h$  as indicated by the shaded square in Figure 1. To be more specific, the velocity at a marker point is interpolated from the surrounding grid points and reversely the force term is distributed back to these grid points.

Traditionally, the marker points are uniformly distributed over the particle surface, which means  $d_m = d_p$ . However, as a consequence of the use of a regularized delta function, the sharp interface of the particle is smeared into a thin spherical shell, and the boundary where the no-slip condition is truly fulfilled departs slightly away from the real particle surface. Consequently, the accuracy of such IBM simulations at a relatively low resolution drops. In this study an optimal  $d_m$  was evaluated for marker points distribution according to the methodology detailed in Tang et al. (2014). The principle of this methodology is that, by locating the marker points slightly inwards the interior of the particle ( $d_m < d_p$ ) as shown in Figure 1, the no-slip boundary condition will be satisfied as close as possible to the particle surface, and consequently the accuracy is improved for predictions of the gas-solid

interactions as well as the flow field. This optimal  $d_m$  was further found to be dependent on the solids volume fraction, the grid resolution and the Reynolds number.

## EXPERIMENTAL TECHNIQUES

### Extended Particle Image Velocimetry

The PIV technique (Bokkers et al., 2004) has been extensively used to measure the instantaneous particle velocity fields in pseudo-2D fluidized beds. A high speed CCD camera is used to record the front view of the bed, which is illuminated using a pair of LED lamps. Two subsequent images of particles, recorded with a short time delay  $\Delta t$ , are divided into small interrogation areas. Cross-correlation analysis is applied to determine the volume-averaged displacement of the particle images within the interrogation areas between the first and second images. Note that outliers are removed with a standard median filter. Subsequently, the solids velocity within the interrogation area is found by dividing this displacement by image magnification and the time delay.

Further, this PIV technique was extended to measure the instantaneous particle granular temperature in gas-fluidized beds. The principle of the extension is Gaussian fitting to the spatial cross-covariance of two subsequent images. Details of this technique can be found in Dijkhuizen et al. (2007).

### Digital Image Analysis

The DIA algorithm is used to compute the instantaneous profile of the solids volume fractions from the images of particles. The digital image consists of pixels with different intensities, distinguishing the particles from the gas phase. After a series of pre-processing steps, namely, background subtraction, elimination of overexposed and underexposed pixels, the image is corrected for inhomogeneity and then normalized between 0 and 1. Here 1 is representative for the brightest particles and 0 for the background or the gas. The normalized values in the 2D image are then averaged over the interrogation areas with the same size as used for PIV to obtain the apparent 2D solids volume fraction. These 2D results are subsequently translated to the 3D solids volume fractions using the correlation proposed by de Jong et al. (2012).

The instantaneous particle velocity vectors obtained from PIV do not account for the number of particles that possess those velocities. When time-averaged velocity profiles are computed using PIV data only, the dynamics of the particles can be misinterpreted, especially because of particle raining through the bubbles, where a small number of particles possess a relatively high velocity, while the particle volumetric flux is small. To correct for this, the instantaneous particle velocity is multiplied with the instantaneous solids volume fraction, followed by averaging over time to obtain the time-averaged volumetric particle flux.

## EXPERIMENTAL/SIMULATION SET-UPS

Simulations and experiments are performed for a pseudo-2D fluidized bed. The sizes of the bed are given in Table 1, together with the properties of the glass particles used in this study. The spherical particles possess a diameter of 2.5 mm and a density of 2526 kg/m<sup>3</sup>, which are Geldart D type particles. The depth of the bed is assumed to be sufficiently small to display pseudo-2D behaviour and is

large enough to avoid extreme particle-wall interaction. For the experiments, the air flow rate was controlled by a digital mass flow controller and supplied at the bottom of the bed through a porous plate gas distributor. To prevent electrostatic build-up, the air was first humidified to 60-70% relative humidity. The pressure drop over the bed was recorded by a high frequency differential pressure sensor, which was connected to the inside bed through a fine wire mesh at the centre of the bed bottom. The minimum fluidization velocity was first measured ( $u_{mf} \approx 1.33$  m/s) by plotting the recorded pressure drop while gradually increasing the superficial gas velocity  $u_g$  in the experiment. Digital images of particles are recorded by a LaVision ImagerPro HS CCD camera with the exposure time set to 1 ms and zero delay time. The frequency with which the PIV image pairs were recorded was 100 Hz. The PIV calculations of the velocity field were conducted with the commercial software package DaVis (LaVision). A multi-pass correlation algorithm was performed using interrogation areas of 64×64 pixels during the first pass and 32×32 pixels with an overlap of 50% during the second pass. Accordingly, the interrogation area of 32×32 pixels was used for DIA and the granular temperature measurements as well.

Parameters	Simulations	Experiments
Bed	100×15×250	100×15×1000
(width×depth×height)	mm <sup>3</sup>	mm <sup>3</sup>
Particle density	2526 kg/m <sup>3</sup>	2526 kg/m <sup>3</sup>
Particle diameter	2.5 mm	2.5 mm
Particle number	5000	5000
Gas density	1.2 kg/m <sup>3</sup>	air
Gas viscosity	1.8×10 <sup>-5</sup> kg/(m·s)	air
Superficial gas velocity $u_g$	2.4 m/s, 2.6 m/s	2.4 m/s, 2.6 m/s
Normal restitution coefficient	0.97	-
Tangential restitution coefficient	0.33	-
Friction coefficient	0.1 (p-p), 0.2 (p-w)	-
Time step	1×10 <sup>-5</sup> s	-

**Table 1:** Parameters used for simulations and experiments of fluidization.

Table 1 also gives the parameters used for our IBM simulations. Note that the height of the entire column (i.e., size of the freeboard) was reduced, in comparison with the height of the experimental set-up, to decrease the computational load. However, exactly the same number of particles were used in the experiments and simulations. For the simulation no-slip boundaries were taken at the walls confining the bed in the lateral directions. Restitution coefficients and friction coefficients corresponding to glass beads were used in the hard-sphere model for particle-particle (p-p) and particle-wall (p-w) collisions. Initially the particle bed was assumed to be at rest. The inflow velocity was specified at the bottom, while a constant pressure outflow boundary condition was used at the top. Simulations were performed at a grid resolution of  $d_p/h=5$ , along with the optimal diameter  $d_m$  of 1.65 mm and 1.6 mm at  $u_g = 2.4$  m/s and  $u_g = 2.6$  m/s, respectively.

## RESULTS

Two sets of experiments and simulations have been conducted at  $u_g = 2.4, 2.6$  m/s, which correspond to  $1.8u_{mf}$  and  $1.95u_{mf}$ , respectively. Similar observations as those discussed in the following sections have also been found for both cases. Thus, we focus on reporting the results for  $u_g = 2.6$  m/s ( $1.95u_{mf}$ ) in this paper.

### Pressure fluctuations

The pressure drop predicted from the IBM simulation is computed as the difference between the pressure at the central point of the bottom plane and the atmosphere pressure. The simulation results are shown in Figure 2a as a function of time, whereas Figure 2b plots a part of the experimental data. It is seen that the time-averaged pressure drop predicted by the simulation is consistent with that measured in the experiment.

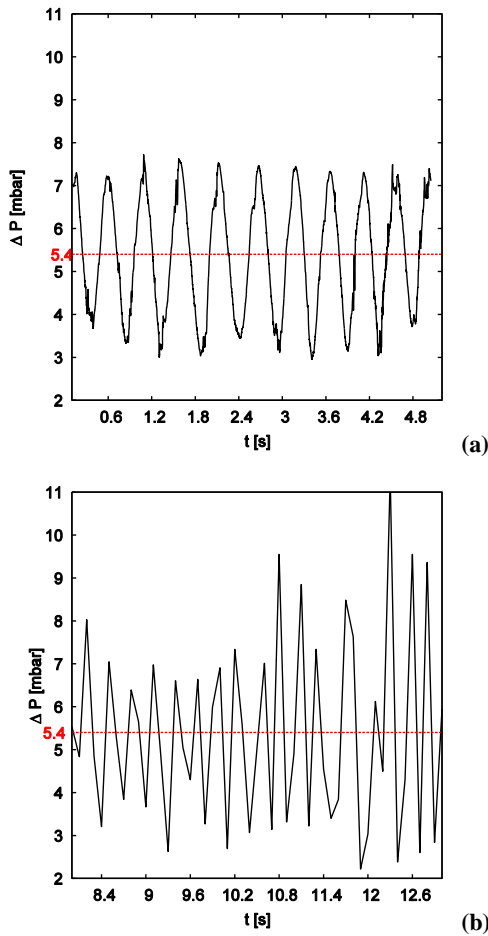


**Figure 2:** Pressure drop as a function of time (a) computed by the IBM simulation, (b) measured in the experiment of fluidization. The red dot lines plot the time-averaged value.

Besides, the fluctuations of pressure drop measured from the experiment turn out to be more complex in comparison with those of simulation data. According to Johnsson et al. (2000) and van Ommen et al. (2011), the simulation results of pressure fluctuations shown in Figure 2a indicate a single bubble regime. Whereas, the pressure fluctuations measured experimentally shown in Figure 2b correspond to a single bubble (8-10.6 s) combined with exploding bubble (10.6-13 s) regime. This difference can be caused by the pressure waves originating from the

bottom of the experimental set-up. For instance, the porous plate at the bottom of the bed cannot possibly provide a perfectly uniform gas distribution as specified in simulations. Consequently, fluctuations occur in the preferred direction of bubble passage. Moreover, in the experiments, the air was humidified by flowing through a vessel of water. This procedure is not exactly stable and might introduce propagating pressure waves from the bottom of the bed.

### Time-averaged solids flux

The filtered time-averaged solids volumetric flux, computed using PIV/DIA based on the experimental images, is shown in Figure 3a, whereas the results obtained from the IBM simulation are shown in Figure 3b. The solids circulation patterns can readily be observed from both results, clearly revealing the existence of two symmetrical vortices with their centres located at a bed height of  $0.045$  m (about  $18d_p$ ). In these circulation patterns, particles move upwards in the centre of the bed and flow downwards close to the side walls. At such an intermediate fluidization velocity ( $1.95u_{mf}$ ), the down-flow regions extend completely down to the distributor. Using the PIV images, we observe that bubbles, after formation at the distributor, move very rapidly towards the centre of the bed and then rise vertically until they erupt at the surface of the particle bed. Thus, the pronounced upward motion of the particles in the central region is induced by the bubble motion. In other words, the particles are carried or driven by the rapidly rising bubbles.

Qualitatively, the solids circulation patterns predicted by the IBM simulation are in agreement with the trend as found experimentally using PIV/DIA measurements. However, one can notice that the time-averaged bed expansion obtained from PIV/DIA is a bit higher than that predicted by the IBM simulation. Some possible reasons for this discrepancy are as follows. First, as discussed above, large exploding bubbles occur in the experiment due to the propagating pressure waves originating from the bottom of the bed, which consequently cause the increase of the bed expansion. Secondly, the DIA algorithm utilizes a correlation to convert the solids volume fractions from 2D to 3D. This correlation was however derived by using discrete element model simulation results, the accuracy of which is *a priori* dependent on the incorporated closures. Therefore, the use of such a correlation might lead to some departure of the 3D results from the true experiment. Furthermore, the collision coefficients used in the IBM simulation are based on reported values in the early work by Hoomans (2000). As is known, the energy dissipation due to the p-p and p-w interactions has a strong influence on the bed behaviour. Consequently, some difference of the predicted solids pattern might result from a slight mismatch of these parameters between simulations and experiments. In addition, we apply an optimal diameter  $d_m$  in the simulation to achieve a better prediction of the gas-solid interaction force. However, the  $d_m$  was found dependent on the grid resolution, the solids volume fraction as well as the mean flow Reynolds number (Tang et al., 2014). In other words, the optimal  $d_m$  for different local particle groups are in principle not the same, due to the distributions of local solids volume fraction and slip velocity in a fluidized bed. Thus, applying a constant  $d_m$  in the entire (heterogeneous) system seems a serious simplification for accurate prediction of the overall gas-solid interaction hence the flow behaviour. In addition,

these parameters ( $\phi$ ,  $Re$ ) are all time-variant in fluidized beds. Apparently from the comparison in Figure 3, the bed expansion might be underestimated by the use of  $d_m = 1.6$  mm during the whole computation.

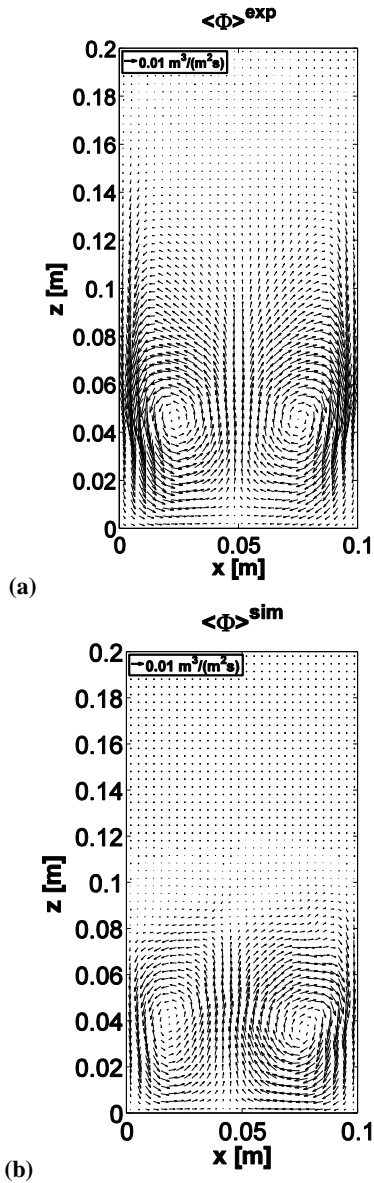


**Figure 3:** Time-averaged solids volumetric flux (a) computed by PIV/DIA from experimental images, (b) calculated from the IBM simulation.

Figure 4 shows the quantitative comparison between the simulation and the experimental results for the lateral profiles of the time-averaged axial solids flux at different heights of the bed. Generally, a good agreement is obtained in this comparison, although some quantitative difference of the bed expansion is found in Figure 3. Besides, the IBM simulation slightly underpredicts the solids flux close to the walls, in comparison with the PIV/DIA results. This observation is consistent with the reason given above with respect to the particle properties like for the p-w interactions used in simulations. Conversely, the mass balance indicated by the lateral summation of the solids flux from PIV/DIA is not satisfied as well as in the simulation results. Again, this observation corresponds to the reason regarding the DIA algorithm

using the 2D to 3D correlation derived on the basis of DEM simulations.

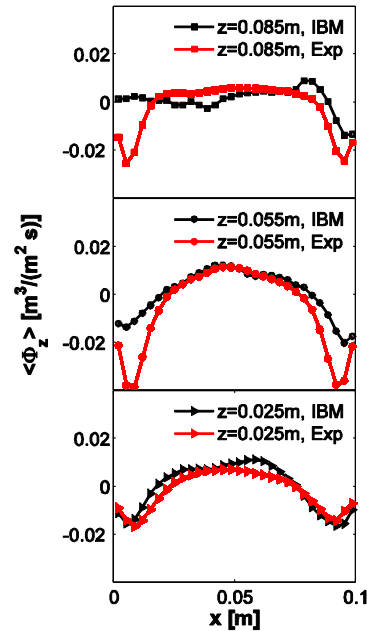


**Figure 4:** Lateral profiles of the time-averaged axial solids flux from the simulation and the experiment at different bed heights.

Nevertheless, both Figure 3 and Figure 4 suggest that a reasonably good agreement has been obtained with respect to the time-averaged solids motion resulted from the IBM simulation and the experimental data. The slight difference of the time-averaged bed expansion is attributed to several reasons in regard to experimental measuring techniques as well as input parameters for the simulations.

#### Granular temperature

As a very important parameter to characterize the flow behaviour in dense gas-fluidized beds, the granular temperature is measured from the experiments and simulations conducted in this study. In terms of the interpretation of two types of granular temperature by Jung et al. (2005), we employ the definition based on local spatial averaging, which corresponds to the particle granular temperature. The experimental measurement was conducted using the extended PIV technique with interrogation areas of  $32 \times 32$  pixels. As for comparison with the experimental 2D measurement, the granular temperature from the IBM simulation is calculated as :

$$\Theta = \frac{1}{2n_p} \sum_{n=1}^{n_p} [\mathbf{v}_n(t) - \langle \mathbf{v}(t) \rangle] \cdot [\mathbf{v}_n(t) - \langle \mathbf{v}(t) \rangle] \quad (1)$$

$$\langle \mathbf{v}(t) \rangle = \frac{1}{n_p} \sum_{n=1}^{n_p} \mathbf{v}_n(t) \quad (1)$$

where,  $\mathbf{v}$  represents particle velocities in directions of the bed width and height. Moreover, similar to the PIV measurement, we divide the computational domain into small windows, which possess a size of  $2d_p$  in each direction. Hereby,  $n_p$  is the number of particles in an individual window.

Figure 5 plots the square root of the mean granular temperature over the particle bed as a function of time

from the experiment, the simulation and the IBM-PIV. For the IBM-PIV calculation, we first create images using different snapshots from the IBM simulation, where the locations of individual particles are provided. In these images, the normalized intensity is between 0 and 1, with 0 representing the gas phase, 1 representing the particles that locate near the front wall of the bed, and values in between representing the rest of particles in terms of their location in bed depth. Subsequently, the granular temperature on the basis of these images is calculated using the extended PIV technique, while applying the same interrogation areas as for the experimental images.

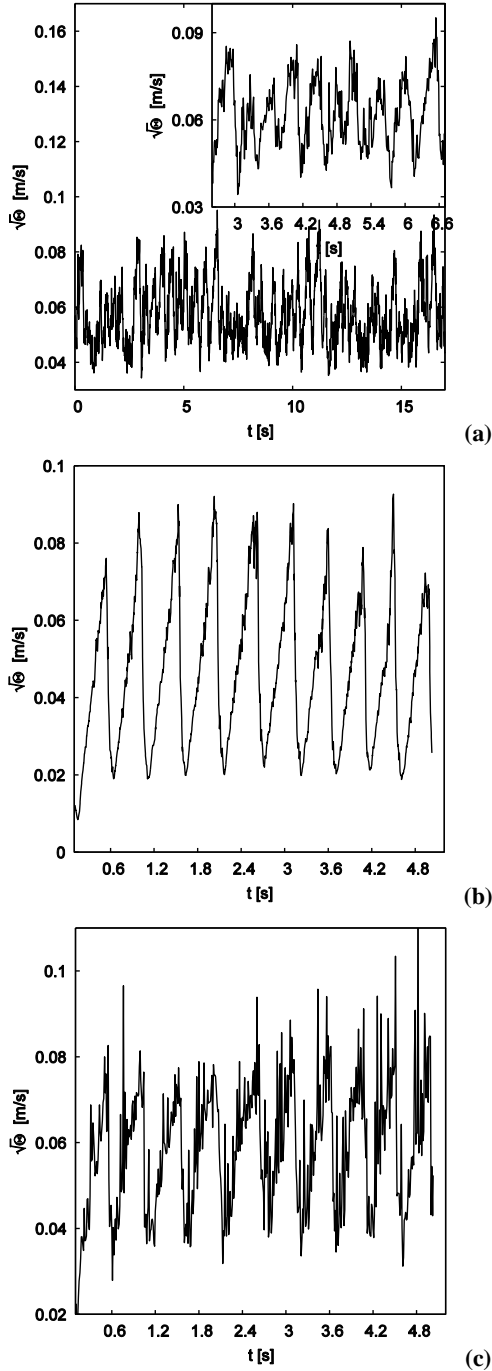


**Figure 5:** Comparison of the square root of the mean granular temperature  $\sqrt{\theta}$  between (a) the experiment, (b) the IBM simulation and (c) the IBM-PIV.

From Figure 5, a very good agreement can be observed on the magnitude as well as the variation of the granular temperature. Furthermore, we also find the same characteristic frequency ( $f = 2 \pm 0.3 \text{ s}^{-1}$ ) of the fluctuations of granular temperature, as shown in the frequency spectra plotted in Figure 6. This also indicates the first successful application of this technique for experimentally measuring the granular temperature in a fully developed gas-fluidized bed, extending the findings of Dijkhuizen et al. (2007).

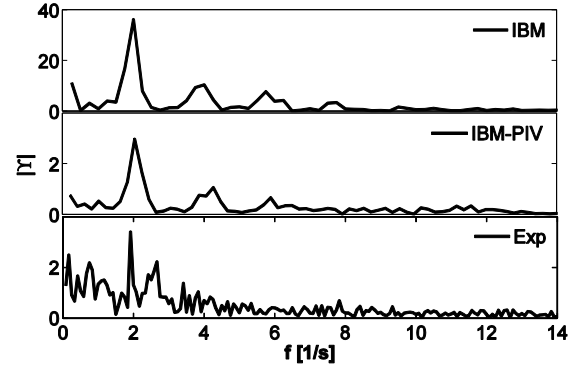


**Figure 6:** The magnitude of the complex Fourier coefficients for the fluctuations in the granular temperature shown in Figure 5.

## CONCLUSION

In this work, we performed direct numerical simulations of realistic fluidization of 5000 particles in a pseudo-2D gas-fluidized bed using an immersed boundary method. The simulation results are directly compared with experimental data for a lab set-up using the extended PIV and DIA techniques. A reasonably good agreement with respect to the time-averaged solids motion is obtained between simulations and experiments, where typical circulation patterns are obtained with the solids moving upwards in the middle of the bed and downwards near the walls. A small difference is observed in the time-averaged bed expansion, which can be attributed to various reasons including simulation input data such as the particle properties and the used constant  $d_m$ , some practical experimental conditions, as well as the 2D to 3D volume correlation used in the DIA algorithm.

Moreover, using the particles images generated from the IBM simulation results, we demonstrate the successful application of the extended PIV technique for measuring the granular temperature in the bubbling fluidization regime. In addition, quantitative agreements have been obtained between our experiments and IBM simulations, with respect to the granular temperature and its spectral characteristics as well.

Finally, we conclude that a successful detailed comparison has been made in this study between DNS and experiments of a pseudo-2D gas-fluidized bed, which has not been reported in literature before.

## ACKNOWLEDGEMENT

The authors would like to thank the European Research Council for its financial support, under its Advanced Investigator Grant scheme, contract number 247298 (Multiscale Flows).

## REFERENCES

- BOKKERS, G.A., VAN SINT ANNALAND, M. AND KUIPERS, J.A.M. (2004), "Mixing and segregation in a bidisperse gas-solid fluidised bed: a numerical and experimental study", *Powder Technol.*, **140**, 176–186.
- DANG, T.Y.N., KOLKMAN, T., GALLUCCI, F. AND VAN SINT ANNALAND, M., (2013), "Development of a novel infrared technique for instantaneous, whole-field, non-invasive gas concentration measurements in gas-solid fluidized beds", *Chem. Eng. J.*, **219**, 545-557.
- DE JONG, J.F., ODU, S.O., VAN BUIJTENEN, M.S., DEEN, N.G., CAN SINT ANNALAND, M. and KUIPERS, J.A.M., (2012), "Development and validation of a novel Digital Image Analysis method for fluidized bed Particle Image Velocimetry", *Powder Technol.*, **230**, 193-202.
- DEEN, N.G., KRIEBITZSCH, S.H.L., VAN DER HOEF, M.A. and KUIPERS, J.A.M., (2012), "Direct numerical simulation of flow and heat transfer in dense fluid-particle systems", *Chem. Eng. Sci.*, **81**, 329–344.
- DEEN, N.G., VAN SINT ANNALAND, M. and KUIPERS, J.A.M., (2004), "Multi-scale modeling of dispersed gas-liquid two-phase flow", *Chem. Eng. Sci.*, **59**, 1853-1861.
- DIJKHUIZEN, W., BOKKERS, G.A., DEEN, N.G., VAN SINT ANNALAND, M. and KUIPERS, J.A.M., (2007), "Extension of PIV for measuring granular temperature field in dense fluidized beds", *AIChE J.*, **53**, 108–118.
- FENG, Z.G. and MUSONG, S.G., (2014), "Direct numerical simulation of heat and mass transfer of spheres in a fluidized bed", *Powder Technol.*, **262**, 62-70.
- HOLLAND, D.J., MÜLLER, C.R., DENNIS, J.S., GLADDEN, L.F. and SEDERMAN, A.J., (2008), "Spatially resolved measurement of anisotropic granular temperature in gas-fluidized beds", *Powder Technol.*, **182**, 171-181.
- HOOMANS, B.P.B., (2000), "Granular Dynamics of Gas-Solid Two-Phase Flows", Ph.D. thesis, Universiteit Twente, Enschede.
- JOHNSSON, F., ZIJERVELD, R.C., SCHOUTEN, J.C., VAN DEN BLEEK, C. and LECKNER, B., (2000), "Characterization of fluidization regimes by time-series analysis of pressure fluctuations", *Int. J. Multiphase Flow*, **26**, 663-715.
- JUNG, J., GIDASPOW, D. and GAMWO, I.K., (2005), "Measurement of two kinds of granular temperatures, stresses, and dispersion in bubbling beds", *Industrial & Engineering Chemistry Research*, **44**, 1329–1341.
- KRIEBITZSCH, S.H.L., VAN DER HOEF, M.A. and KUIPERS, J.A.M., (2013), "Fully resolved simulation of a gas-fluidized bed: A critical test of DEM models", *Chem. Eng. Sci.*, **91**, 1–4.
- KUWAGI, K., UTSUNOMIYA, H., SHIMOYAMA, H.H.Y. and TAKAMI, T. (2010), "Direct numerical simulation of fluidized bed with immersed boundary method, *The 13th International Conference on Fluidization-New Paradigm in Fluidization Engineering*, RP6, Korea.
- LAVERMAN, J.A., ROGHAI, I., VAN SINT ANNALAND, M. and KUIPERS, J. A. M., (2008), "Investigation into the hydrodynamics of gas-solid fluidized beds using particle image velocimetry coupled with digital image analysis", *The Canadian Journal of Chemical Engineering*, **86**, 523–535.
- MÜLLER, C.R., HOLLAND, D.J., SEDERMAN, A.J., SCOTT, S.A., DENNIS, J.S. and GLADDEN, L.F., (2008), "Granular temperature: Comparison of magnetic resonance measurements with discrete element model simulations", *Powder Technol.*, **184**, 241-253.
- PAN, T.-W., JOSEPH, D.D., BAI, R., GLOWINSKI, R. and SARIN, V., (2002), "Fluidization of 1204 spheres: simulation and experiment", *J. Fluid Mech.*, **451**, 169–191.
- PATIL, A.V., PETERS, E.A.J.F., SUTKAR, V.S., DEEN, N.G. and KUIPERS, J.A.M., (2015), "A study of heat transfer in fluidized beds using an integrated DIA/PIV/IR technique", *Chem. Eng. J.*, **259**, 90-106.
- TANG, Y., KRIEBITZSCH, S.H.L., PETERS, E.A.J.F., VAN DER HOEF, M.A. and KUIPERS, J.A.M., (2014), "A methodology for highly accurate results of direct numerical simulations: Drag force in dense gas-solid flows at intermediate Reynolds number", *Int. J. Multiphase Flow*, **62**, 73–86.
- TANG, Y., KRIEBITZSCH, S.H.L., PETERS, E.A.J.F., VAN DER HOEF, M.A. and KUIPERS, J.A.M., (2015), "A new drag correlation from fully resolved simulations of flow past monodisperse static arrays of spheres", *AIChE J.*, **61**, 688–698.
- VAN DER HOEF, M.A., VAN SINT ANNALAND, M., DEEN, N.G. and KUIPERS, J.A.M., (2008), "Numerical simulation of dense gas-solid fluidized beds: A multiscale modeling strategy", *Annu. Rev. Fluid Mech.*, **40**, 47–70.
- VAN DER HOEF, M.A., VAN SINT ANNALAND, M. and KUIPERS, J.A.M., (2004), "Computational fluid dynamics for dense gas-solid fluidized beds: a multi-scale modeling strategy", *Chem. Eng. Sci.*, **59**, 5157–5165.
- VAN OMMEN, J.R., SASIC, S., VAN DER SCHAAF, J., GHEORGHIU, S., JOHNSSON, F. and COPPENS, M.O., (2011), "Time-series analysis of pressure fluctuations in gas-solid fluidized beds-A review", *Int. J. Multiphase Flow*, **37**, 403- 428.